OAK RIDGE NATIONAL LABORATORY LIBRARIES
3 4456 0593047 3

CRL

145

CENTRAL RESEARCH LIBRARY
DOCUMENT COLLECTION

ORNL-2433
UC-4 – Chemistry-General
TID-4500 (15th ed.)

# FUSED SALT HEAT TRANSFER – PART III: FORCED-CONVECTION HEAT TRANSFER IN CIRCULAR TUBES CONTAINING THE SALT MIXTURE $NaNO_2$-$NaNO_3$-$KNO_3$

H. W. Hoffman
S. I. Cohen

CENTRAL RESEARCH LIBRARY
DOCUMENT COLLECTION
LIBRARY LOAN COPY
DO NOT TRANSFER TO ANOTHER PERSON
If you wish someone else to see this document, send in name with document and the library will arrange a loan.

OAK RIDGE NATIONAL LABORATORY
operated by
UNION CARBIDE CORPORATION
for the
U.S. ATOMIC ENERGY COMMISSION

Printed in USA. Price $1.00. Available from the

Office of Technical Services
Department of Commerce
Washington 25, D.C.

LEGAL NOTICE

This report was prepared as an account of Government sponsored work. Neither the United States, nor the Commission, nor any person acting on behalf of the Commission:

A. Makes any warranty or representation, expressed or implied, with respect to the accuracy, completeness, or usefulness of the information contained in this report, or that the use of any information, apparatus, method, or process disclosed in this report may not infringe privately owned rights; or

B. Assumes any liabilities with respect to the use of, or for damages resulting from the use of any information, apparatus, method, or process disclosed in this report.

As used in the above, "person acting on behalf of the Commission" includes any employee or contractor of the Commission, or employee of such contractor, to the extent that such employee or contractor of the Commission, or employee of such contractor prepares, disseminates, or provides access to, any information pursuant to his employment or contract with the Commission, or his employment with such contractor.

ORNL-2433

Contract No. W-7405-eng-26

REACTOR EXPERIMENTAL ENGINEERING DIVISION

# FUSED SALT HEAT TRANSFER – PART III: FORCED-CONVECTION HEAT TRANSFER IN CIRCULAR TUBES CONTAINING THE SALT MIXTURE $NaNO_2$-$NaNO_3$-$KNO_3$

H. W. Hoffman
S. I. Cohen

DATE ISSUED

MAR -1 1960

OAK RIDGE NATIONAL LABORATORY
Oak Ridge, Tennessee
operated by
UNION CARBIDE CORPORATION
for the
U. S. ATOMIC ENERGY COMMISSION

OAK RIDGE NATIONAL LABORATORY LIBRARIES

3 4456 0593047 3

## CONTENTS


Abstract ..... 1

Introduction ..... 1

Description of Apparatus ..... 3

Results ..... 7

System Calibration ..... 7

Analysis ..... 7

Results ..... 8

Discussion ..... 10

Conclusions ..... 12

Acknowledgment ..... 13

Appendix A. Physical Properties of HTS ..... 15

Appendix B. Experimental Data ..... 17

Appendix C. Recalculation of Data Obtained by Kirst, Nagle, and Castner ..... 21

Nomenclature ..... 22

References Cited ..... 23

# FUSED SALT HEAT TRANSFER – PART III: FORCED-CONVECTION HEAT TRANSFER IN CIRCULAR TUBES CONTAINING THE SALT MIXTURE $NaNO_2$-$NaNO_3$-$KNO_3$

H. W. Hoffman S. I. Cohen


## ABSTRACT

Experimental heat-transfer coefficients were determined for the molten salt mixture $NaNO_2$-$NaNO_3$-$KNO_3$ (40-7-53 wt %) flowing by forced convection through circular tubes. The variables ranged as follows:

| | |
|---|---|
| Reynolds modulus | 4850–24,710 |
| Prandtl modulus | 4.2–9.1 |
| Average fluid temperature, °F | 552–828 |
| Heat flux, $Btu \cdot hr^{-1} \cdot ft^{-2}$ | 62,800–194,500 |

Within this set of conditions, the heat-transfer coefficient varied from 800 to 2900 $Btu \cdot hr^{-1} \cdot ft^{-2} \cdot (°F)^{-1}$ ($N_{Nu}$ from 35 to 125). It was concluded that heat transfer with this salt could be represented by the general correlations for forced-convection heat transfer with normal fluids ($0.5 < N_{Pr} < 100$) flowing in circular ducts. A cooling-effectiveness comparison showed tenfold-greater pumping power requirements for this salt than for a number of other molten salts and liquid metals. This, in combination with susceptibility to nuclear-radiation damage, indicates that the use of this nitrate-nitrite salt mixture may be limited to secondary cooling circuits or to the high-temperature, noncorrosive testing of simulated reactor systems.


## INTRODUCTION

The high temperature levels and heat fluxes associated with modern industrial processes and with many nuclear reactor systems have occasioned considerable interest in such high-efficiency coolants as the liquid metals and fused salts. By virtue of their nonflammability, low vapor pressures, possible multifunctional use as moderator, fuel-carrier, and coolant, and their ready adaptability to continuous fuel processing, the fused salts have shown to particularly good advantage for reactor application. The Aircraft Reactor Experiment, operated at the Oak Ridge National Laboratory in 1955 with an NaF-$ZrF_4$-$UF_4$ mixture as the coolant-fuel, may be considered the precursor of such reactor types (*1*). More recently, substantial effort has been expended on the application of molten-salt systems to the production of commercial atomic power (*2*).

With such usage in mind, then, this Laboratory has been investigating the heat-transfer characteristics of molten salts and hydroxides (*3*, *4*), typical among these being sodium hydroxide, the LiF-NaF-KF (46.5-11.5-42.0 mole %) eutectic, and NaF-$ZrF_4$-$UF_4$ (50-46-4 mole %). While these experiments have indicated that the molten salts have the heat-transfer properties of normal fluids ($0.5 < N_{Pr} < 100$), these same studies have also shown that phenomena such as nonwetting and interfacial film formation can drastically reduce the heat transfer. Since these effects are difficult to predict, the heat-transfer characteristics of the molten salts for critical applications should be experimentally established.

This report describes the heat transfer with a eutectic mixture of $NaNO_3$-$KNO_3$-$NaNO_2$ (7-53-40 wt %), which has a melting point of 288°F. The commercial designation of this salt is HTS (heat transfer salt); this terminology will be used in the remainder of this report. HTS is usable to temperatures of about 1000°F, at which point some decomposition begins. Because of its low melting temperature, there is some interest in this salt as a secondary coolant. Being water soluble

and essentially noncorrosive, HTS can also be used as a medium for observing the high-temperature operation of heat-transfer loops and simulated reactor systems.

Heat-transfer and thermal-property measurements with HTS were first reported in 1940 by Kirst, Nagle, and Castner (5). These authors also investigated the corrosion, thermal stability, and handling of this salt mixture. Additional physical-property data appeared in the Russian literature (6) in 1952. Hoffman (7) in 1955 reported some physical-property checks and preliminary heat-transfer data along with the results of an investigation of the nuclear-radiation stability of HTS. Pertinent conclusions of some of these studies are summarized in the following paragraphs.

The corrosive effect of HTS on a number of common structural materials was determined by Kirst, Nagle, and Castner by suspending weighed samples of known area in the liquid, which was either quiet or gently agitated. Their results showed that, after exposures at temperatures between 850 and 1000°F for periods up to six weeks, materials such as 15% chromium iron, 18-8% chrome nickel with 1% niobium, and 18-8% chrome nickel with 2–4% molybdenum were not corroded. Low-chromium steels containing aluminum, silicon, and molybdenum showed as much as 6–12 mpy attack at 1000°F. Among the nonferrous metals and alloys tested at 1000°F, copper corroded at a rate of 360 mpy and Monel at 1.2 mpy, and Inconel showed no attack. While some additional study of corrosion and mass transfer with HTS may be necessary, it appears that the metals now commonly used for reactor structural materials are compatible with HTS.

Thermal stability studies have indicated that HTS is very stable at temperatures up to 800°F and can be expected to give excellent service for many years. Above 1100°F the salt undergoes a slow decomposition in accord with the reaction

$$5NaNO_2 \longrightarrow 3NaNO_3 + Na_2O + N_2$$

resulting in a gradual rise in the melting temperature. In the presence of air, the reaction

$$2NaNO_2 + O_2 \longrightarrow 2NaNO_3$$

has also been observed. The quantity of makeup salt required will depend on the application, the temperature, and the length of exposure to elevated temperatures.

HTS introduces no hazards, in the absence of foreign materials, beyond those associated with ordinary liquids at high temperatures. High pressures are not required, and no toxic vapors are evolved. However, based on the tests of Kirst *et al.* (5), safety precautions should begin with the assumption that, while organic matter will react with the salt to evolve the normal gases of combustion ($N_2$, $CO_2$, and $H_2O$), traces of poisonous gases such as CO and NO will also be formed. Explosions of large, pure nitrate baths used in the treatment of aluminum have been reported abroad; however, the aluminum industry in this country has had many years of relatively satisfactory experience with the heat treatment of aluminum alloys in fused nitrate baths. It is believed that the high percentage of nitrite present in the HTS mixture inhibits the explosive reaction. Kirst, Nagle, and Castner examined some materials and mixtures at temperatures as high as 1200°F without any indication of the violent reactions reported. Indeed, attempts to detonate HTS and HTS-paraffin mixtures at temperatures up to 1100°F have been unsuccessful.

Three samples of HTS were irradiated in this Laboratory by O. Sisman to establish the nuclear radiation stability of the salt. The samples received a thermal dose of $3.3 \times 10^{18}$ neutrons/cm$^2$ and an epithermal dose of somewhat less than half the thermal dose. Examination of the irradiated samples indicated that the salt is rendered more hygroscopic by radiation and that it also undergoes some breakdown, yielding, in part, gaseous decomposition products.

The breakdown of HTS as the result of high temperatures and nuclear radiation complicates the use of this salt for reactor applications. Thus facilities would be required for gas removal and for the reconversion of the alkali formed to either the nitrite or the nitrate (by treatment of a bypass stream with $N_2O_5$ or $N_2O_3$). Periodic addition of new salt of such composition as to return the mixture to its original constitution (and original melting point) would also be necessary. In this aspect, the use of HTS would appear to pose engineering and chemical problems of no greater difficulty than those existing in reactor designs employing high-boiling organic fluids as coolants.

## DESCRIPTION OF APPARATUS

The apparatus used for determination of the heat-transfer coefficients for HTS is essentially as described in earlier reports on similar measurements with NaOH (*3*) and the eutectic named Flinak, LiF-NaF-KF (46.5-11.5-42.0 mole %). Only those modifications specific to this experiment will be described in detail in this section.

The essentials of the system are shown in Figs. 1 and 2. Heat was transferred uniformly to the salt as it flowed under gas pressure through an electrical-resistance-heated test section connecting two tanks. The inlet and outlet mixed-mean fluid temperatures, the temperature of the outer surface of the tube, the electrical power input, and the fluid flow rate were measured. Helium, treated by passage through silca gel and heated titanium sponge to remove residual oxygen and water vapor, was used as the pressurizing and blanket gas.

All system components were fabricated from Inconel and welded together to form a gastight, essentially integral unit. The weigh and sump tanks (right circular cylinders of 8-in. ID and 12-in. height) represent one major change from the previous systems, being so reduced in size that the salt inventory was only 10% of that used in the earlier studies. While this decreased the cost of the system and of the salt required, the change added several new, though easily surmountable, complications. For example, operational times were shortened from 20 to 30 min per run to 1 to 1 ½ min per run. It therefore became necessary to simultaneously record selected tube-surface temperatures and the inlet and outlet mixed-mean temperatures. Since the mass of the weigh tank was no longer sufficient to eliminate the effect of the rest of the system on the weight measurement, a flexible, thin-metal bellows was provided to isolate the dip line from the weigh

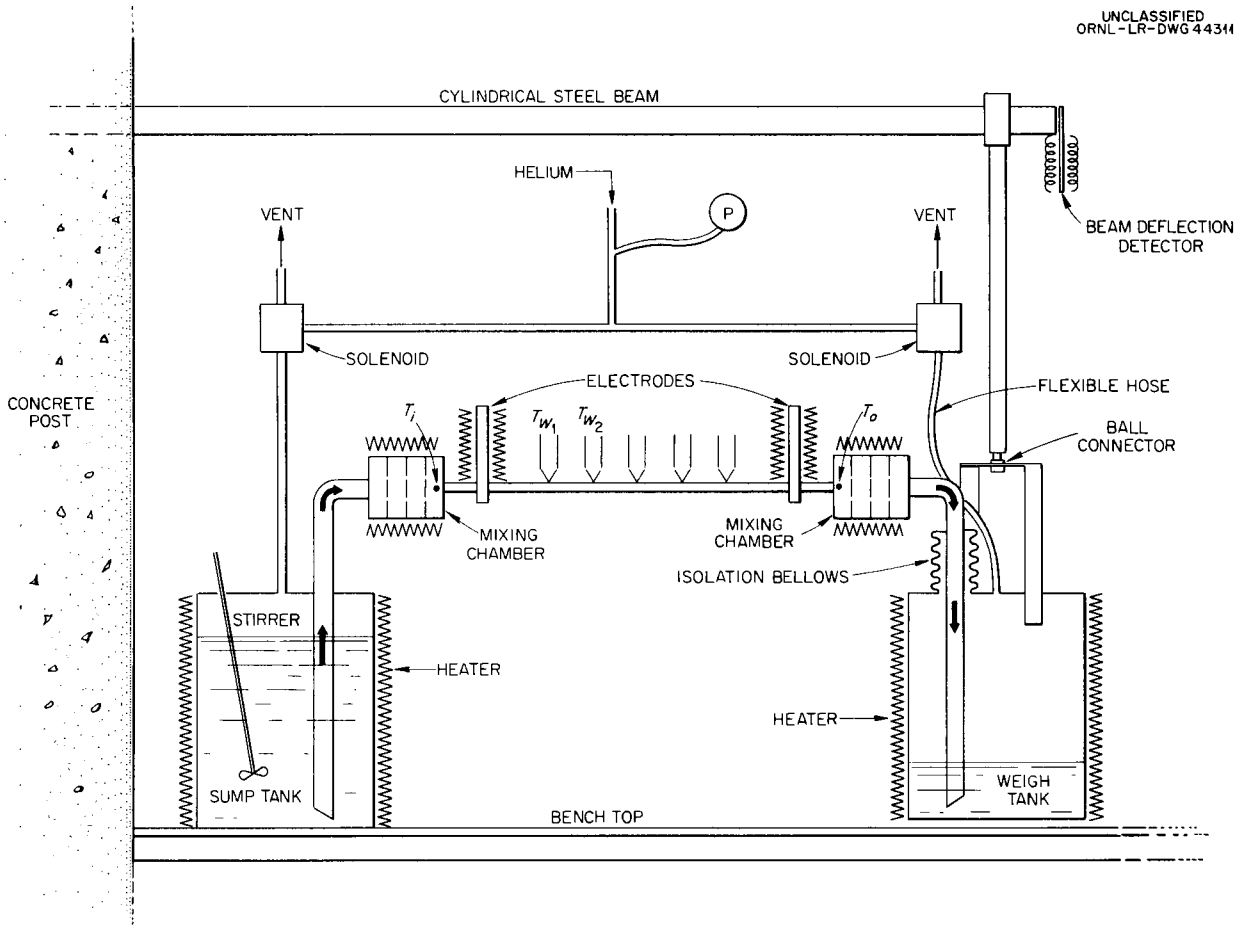


**Fig. 1. Diagram of System.**

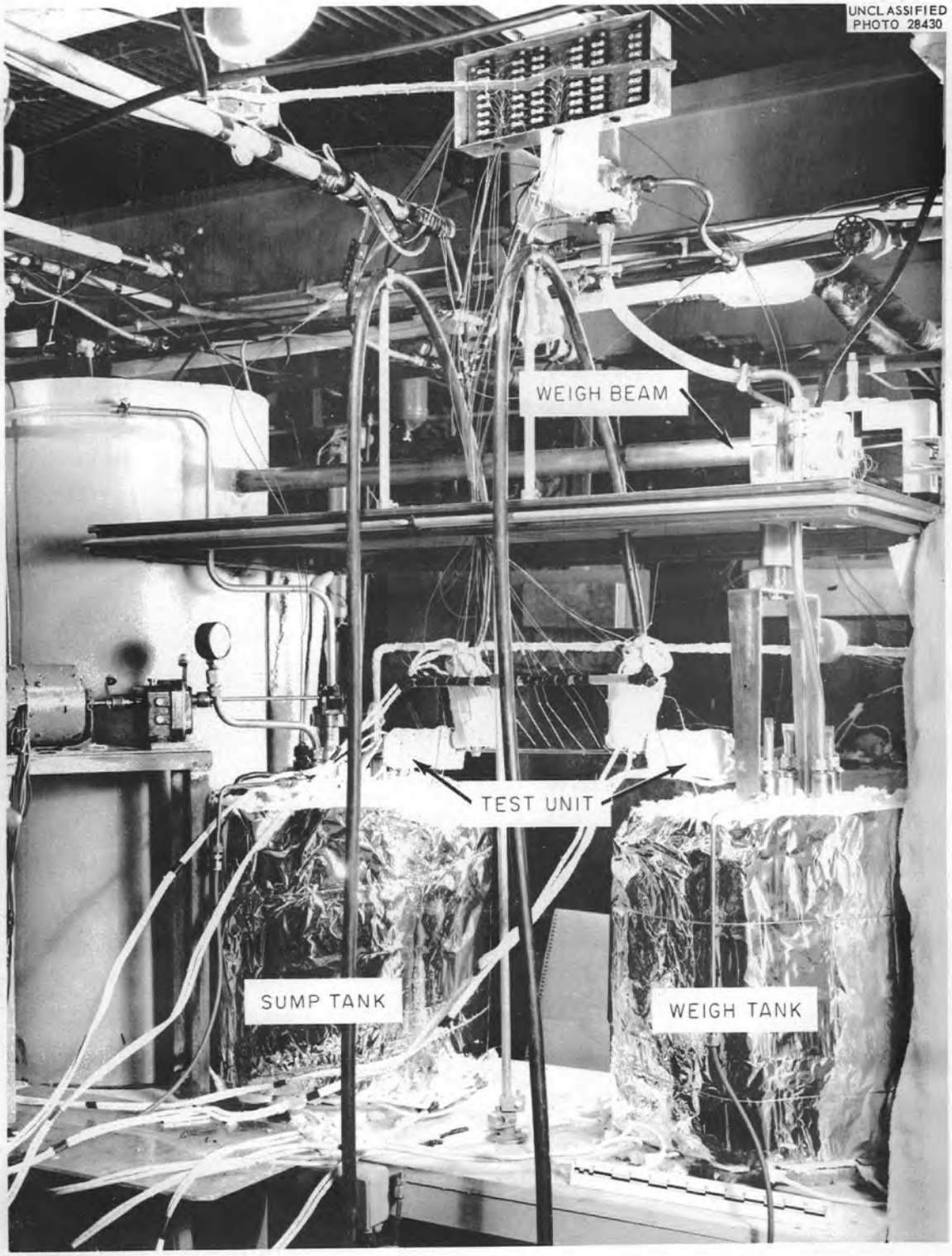


**Fig. 2. HTS Heat-Transfer System with Test Unit Uninsulated.**

tank. Linear thermal expansion of the test section was also absorbed by this bellows; the thermal expansion problem was further alleviated by reducing the test-section length to about 10 in.

Flow rates were obtained by a weight method involving the calibrated deflection of a cantilever beam from which the tank was freely suspended (see Figs. 1 and 2). The movement of the unsupported end of the beam was detected by a sensitive microformer (a differential transformer with a movable iron core) and recorded on a Brown 5-mv instrument. The measuring system could be adjusted to give full-scale displacement for any desired quantity of salt transferred. While the system was capable of sensing weight changes of as little as 0.002 lb, it was found that a sensitivity of 0.2 lb was sufficient. Calibration of the weigh beam was effected by flowing lead shot into a container resting on the beam. A signal from the weight recording instrument (triggered when preset maximum and minimum values for the amount of salt in the tank were reached) was used to operate the solenoid valves supplying the pressurizing gas.

The test section, typically an Inconel tube having a 0.035-in. wall, an outside diameter of $\frac{1}{4}$ in., and a length of 9.5 in. ($x/d = 52.8$), was heated by passing an electric current through the tube wall. The power was supplied by a 7.5-kva transformer and was transmitted to the tube through Inconel electrodes Nicrobrazed to the tube at each end. Thermocouples of 36-gage Chromel-Alumel duplex wire were resistance welded to the tube at approximately 1-in. intervals along the length, as shown in Fig. 3. Fluid mixed-mean inlet and outlet temperatures were obtained in mixing chambers

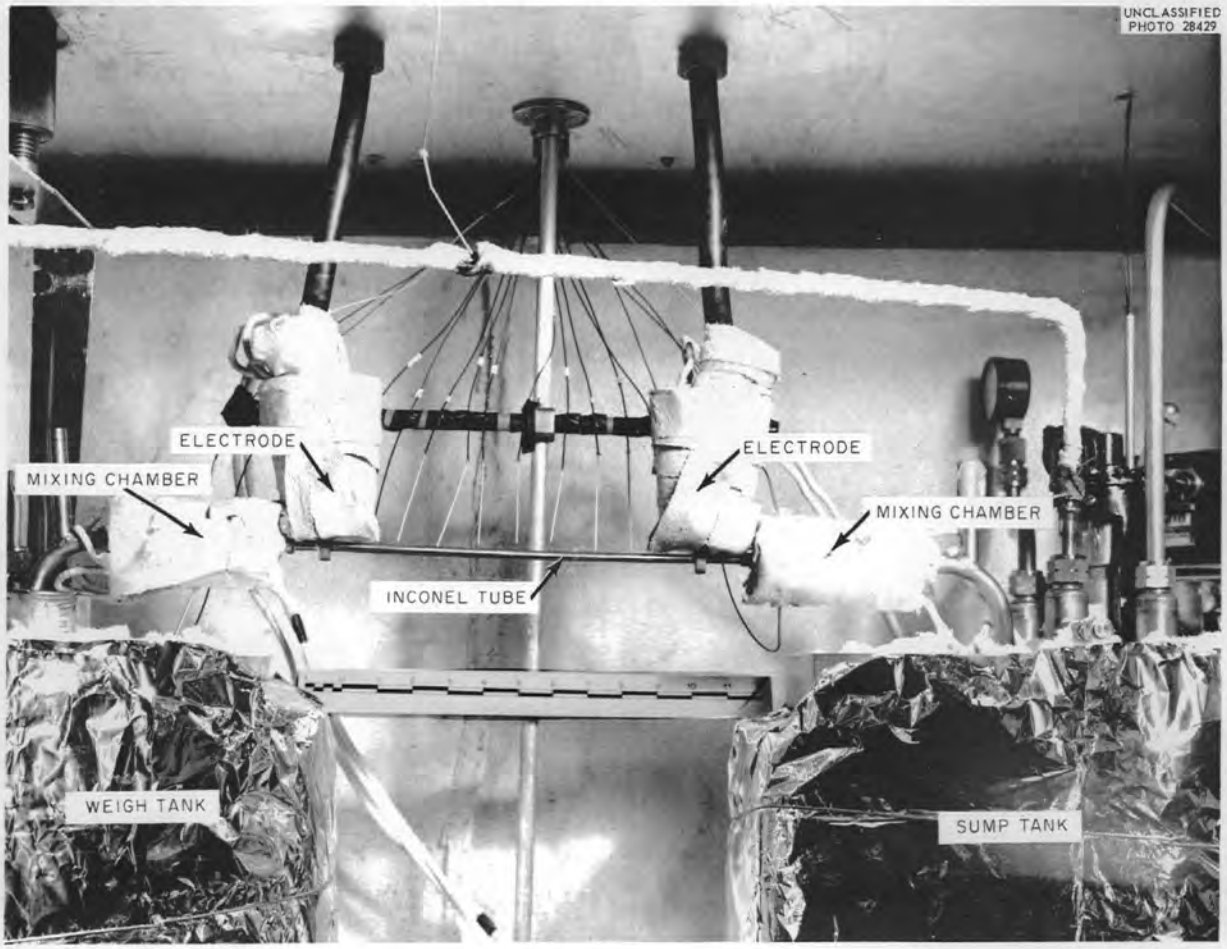


**Fig. 3. Close-Up of Test Unit Showing Electrodes and Mixing Chambers with Guard Heaters Installed.**

of "disk-and-donut" design, located at the tube ends, by means of a pair of 36-gage thermocouples in each mixing pot. Independently controlled clamshell heaters were used to minimize heat losses from the electrodes and mixing chambers. The entire test unit was encased by a metal box containing a loose, high-temperature insulating material.

The desired temperature levels were established by heaters jacketing the weigh and sump tanks. Constancy of the temperature of the salt entering the test section during a run was maintained by a stirrer located in the sump tank. Results were obtained only during transfers from the sump to the weigh tank, since the baffle-thermowell arrangement in the mixing chambers yielded valid mixed-mean fluid temperatures for flows in this direction only.

Pertinent features of the control and data recording system are indicated in Fig. 4.

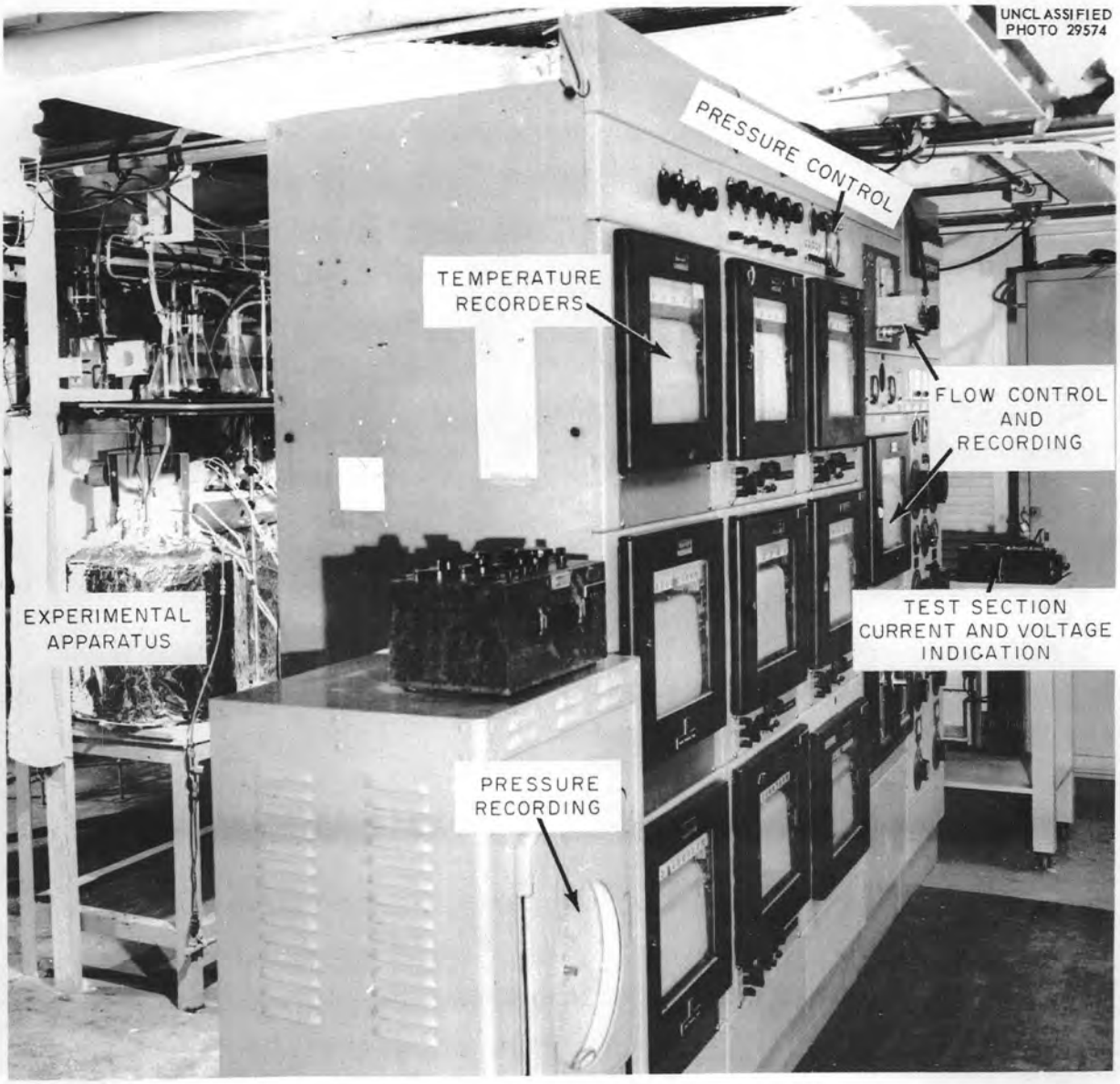


**Fig. 4. Instrument Panel for HTS Heat-Transfer System.**

## RESULTS

### System Calibration

Calibration of essential system components was accomplished as in the earlier studies with NaOH and Flinak. This included system-heat-loss determination and thermocouple calibration. Typical of the axial variation in the outer-tube-surface temperatures during heat-loss operation is that shown in Fig. 5 for the test series AD. In this technique of heat-loss operation, the tube is heated without fluid flow; hence, the entire energy input goes into heat loss. Further, since all guard heaters are set at projected operating levels, the calibration includes electrode and end losses. The heat loss at a given average tube-surface temperature (obtained by graphical integration of the curves of Fig. 5) is then expressed as the equilibrium power input for a given average temperature difference between the tube outer wall and the system environment. This is presented in Fig. 6. The nonlinear relationship observed probably results from the changing natural convection pattern around the test unit as the average tube temperature increases.

A question of major importance is the approach to thermal equilibrium during the 1- to 1½-min flow time of a run. That equilibrium was achieved is attested by the curves of Fig. 7, which show a typical set of tube-surface and fluid-mean temperatures. Following changes in the test-section

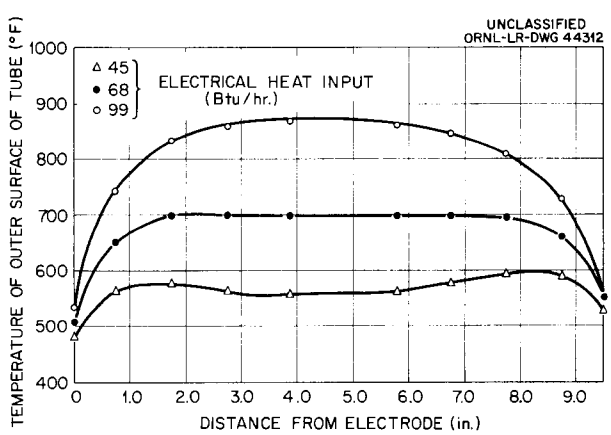


**Fig. 5. Axial Profiles of Temperatures of Outer Surface of Tube for Varying Heat Input with No Fluid Flow.**

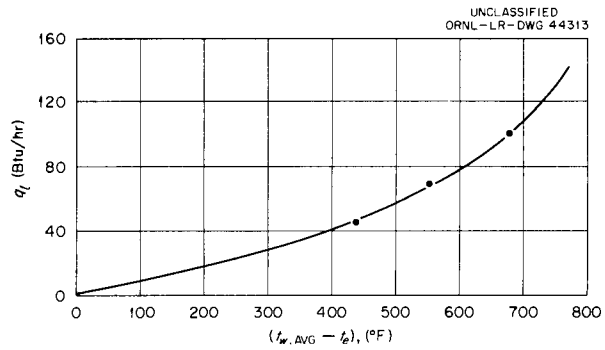


**Fig. 6. System Heat Loss.**

power input, it was necessary to cycle the fluid for about 5 min to establish new equilibrium temperature profiles in the insulation around the test section.

### Analysis

The local coefficient of convective heat transfer is defined by the equation

$$h_x = \frac{(q_l/A_s)_x}{(t_s - t_m)_x} , \qquad (1)$$

where $x$ is the position on the surface at which the heat flux and temperature difference are evaluated. For flow in a tube, $x$ is the distance from the beginning of the heated section. At large values of $x$ (i.e., beyond the thermal and hydrodynamic entrance regions), $h_x$ assumes a limiting value, $h$. In this experiment, the temperatures were taken sufficiently far downstream to ensure location in this region of established turbulent flow; hence, $h$ is the quantity correlated. The previous data for Flinak and NaOH yielded thermal entrance lengths of 20 to 40 tube diameters for the range of the Peclet modulus covered in this experiment. Generally, the surface temperatures here measured were for $x/d_e$ values in excess of 30, although the axial temperature profile data obtained do indicate the possibility of shorter thermal entrance regions for HTS. This point was not specifically determined in this study.

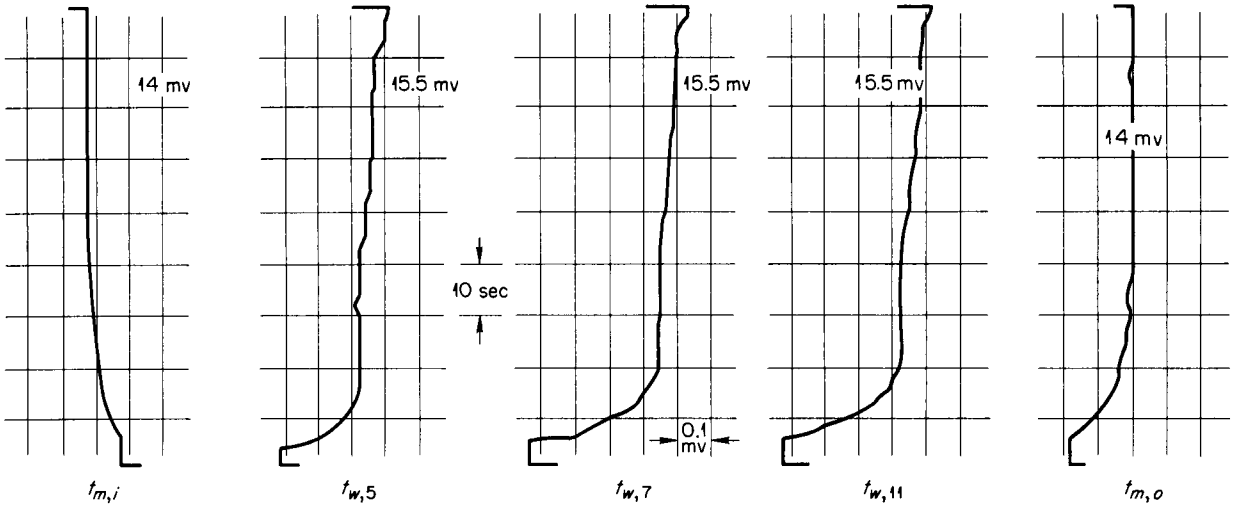


**Fig. 7. Typical Thermocouple Traces: Run AD-18.**

The inner-tube-surface temperature can be related to the measured outer-tube-surface temperature by the equation

$$t_w - t_s = \frac{W}{2k_m}\left(r_w^2 \ln \frac{r_w}{r_s} - \frac{r_w^2 - r_s^2}{2}\right) , \qquad (2)$$

which is the modification of the simple conduction equation allowing for the generation of heat in the tube wall. The derivation of this equation is given in ref (*3*). The source term, $W$, is given by

$$W = \frac{3.413EI}{V} . \qquad (3)$$

In the derivation of Eq. (3), it was assumed that there existed uniform heat generation in the tube wall, no longitudinal heat flow, and zero losses through the outer surface. The first of these assumptions was verified by the observation of the linear variation of the voltage along the tube length (*3*, *4*). Analysis, based on the experimental temperature profiles, has shown that longitudinal heat flow was significant only in the immediate vicinity of the electrodes, even then representing, at most, only 0.2% of the total heat flow. Similarly, from the heat-loss calibration previously described, the outward flow of heat to the environment was found to be in most cases less than 5% of the net heat transferred to the salt passing through the tube; this loss was generally ignored in determining the temperature of the inner surface of the tube. Thus a typical calculation, in which the heat-loss term was included in Eq. (2), yielded a correction to the temperature drop across the wall of less than 0.1°F.

The heat gained by the fluid in traversing the test section is given by

$$q_f = wc_p\,(t_{m,o} - t_{m,i}) . \qquad (4)$$

Since the axial temperature rise of the fluid is relatively small (allowing temperature dependence of the physical properties of the salt to be neglected) and the heat is being uniformly transferred, the temperature of the fluid can be taken to vary linearly from the inlet to the exit.

The surface heat flux was based on the convective heat gain of the fluid [Eq. (4)] and the inner surface area of the tube between electrodes. The thermal properties necessary to the analysis of the data are given in Appendix A.

## Results

The data were evaluated as the Colburn $j$ function, a dimensionless heat-transfer modulus having the form

$$j = N_{\mathrm{St}}N_{\mathrm{Pr}}^{2/3} = \frac{N_{\mathrm{Nu}}}{N_{\mathrm{Re}}N_{\mathrm{Pr}}}N_{\mathrm{Pr}}^{2/3}$$

$$= \left(\frac{h}{c_pG}\right)\left(\frac{c_p\mu}{k}\right)^{2/3} . \qquad (5)$$

The results are given in Table 1 and graphed in Fig. 8 along with a recalculation of the Kirst, Nagle, and Castner data, which will be discussed in the next section. The temperatures, flow rates, and other quantities pertinent to the reduction of the data are tabulated in Appendix B. Also given in Appendix B are the Kirst, Nagle, and Castner results and a typical axial temperature profile. In view of the small magnitude of the heat losses, the heat balances have been expressed as the ratio of the convective heat gain to the electrical energy input. Comparison has been made with the

**Table 1. Results of Heat-Transfer Studies with Molten HTS**

| Run | $N_{Re}$ | $N_{Pr}$ | $N_{Nu}$ | $N_{St}$ | $j$ | $N_{Nu}/N_{Pr}^{0.4}$ |
|---|---|---|---|---|---|---|
| AB 6 | 7,300 | 6.4 | 48.0 | 0.00103 | 0.00354 | 22.9 |
| 10 | 7,950 | 7.9 | 57.4 | 0.00092 | 0.00364 | 25.1 |
| 11 | 8,200 | 7.6 | 57.4 | 0.00043 | 0.00357 | 25.6 |
| 17 | 10,100 | 7.4 | 71.4 | 0.00096 | 0.00361 | 32.1 |
| 21 | 7,970 | 6.8 | 52.7 | 0.00097 | 0.00349 | 24.5 |
| 22 | 11,200 | 6.3 | 71.6 | 0.00111 | 0.00379 | 34.3 |
| 29 | 10,400 | 5.9 | 72.9 | 0.00119 | 0.00387 | 35.9 |
| 31 | 12,100 | 5.8 | 82.3 | 0.00118 | 0.00381 | 40.7 |
| 32 | 10,400 | 6.0 | 74.6 | 0.00122 | 0.00401 | 36.5 |
| 34 | 8,810 | 5.6 | 58.5 | 0.00118 | 0.00375 | 29.3 |
| AC 10 | 9,900 | 5.3 | 62.1 | 0.00118 | 0.00360 | 31.8 |
| 11 | 10,340 | 6.4 | 72.0 | 0.00109 | 0.00376 | 34.3 |
| 12 | 10,650 | 6.3 | 71.6 | 0.00107 | 0.00365 | 34.3 |
| 13 | 7,350 | 5.8 | 53.1 | 0.00125 | 0.00404 | 26.3 |
| 14 | 8,590 | 5.4 | 54.6 | 0.00117 | 0.00362 | 27.8 |
| 15 | 9,700 | 5.3 | 63.0 | 0.00122 | 0.00372 | 32.2 |
| 16 | 9,840 | 5.3 | 63.9 | 0.00122 | 0.00372 | 32.7 |
| 17 | 11,300 | 5.3 | 72.6 | 0.00121 | 0.00369 | 37.2 |
| AD 1 | 10,490 | 7.8 | 86.9 | 0.00106 | 0.00418 | 38.1 |
| 3 | 11,330 | 7.6 | 88.2 | 0.00103 | 0.00397 | 39.3 |
| 4 | 11,740 | 7.4 | 92.4 | 0.00106 | 0.00403 | 41.5 |
| 5 | 12,070 | 7.3 | 96.9 | 0.00110 | 0.00414 | 43.8 |
| 6 | 12,600 | 7.1 | 97.0 | 0.00108 | 0.00401 | 44.2 |
| 7 | 12,630 | 7.1 | 97.8 | 0.00108 | 0.00401 | 44.6 |
| 8 | 12,870 | 7.0 | 106.5 | 0.00118 | 0.00433 | 48.8 |
| 9 | 12,280 | 7.0 | 91.2 | 0.00106 | 0.00387 | 41.9 |
| 10 | 12,280 | 7.0 | 97.2 | 0.00113 | 0.00412 | 44.7 |
| 11 | 12,480 | 6.9 | 89.1 | 0.00104 | 0.00375 | 41.2 |
| 12 | 13,330 | 6.8 | 98.2 | 0.00109 | 0.00390 | 45.7 |
| 13 | 10,160 | 6.8 | 78.0 | 0.00113 | 0.00405 | 36.3 |
| 14 | 10,110 | 6.7 | 83.4 | 0.00123 | 0.00438 | 39.0 |
| 15 | 10,370 | 6.7 | 85.0 | 0.00123 | 0.00435 | 39.8 |
| 16 | 10,770 | 6.6 | 89.9 | 0.00126 | 0.00444 | 42.3 |
| 17 | 9,810 | 6.6 | 78.9 | 0.00123 | 0.00431 | 37.2 |
| 18 | 10,350 | 6.5 | 80.0 | 0.00119 | 0.00414 | 37.8 |
| 19 | 10,520 | 6.4 | 73.8 | 0.00110 | 0.00380 | 35.1 |
| 20 | 10,500 | 6.3 | 69.4 | 0.00105 | 0.00358 | 33.3 |
| 21 | 10,600 | 6.2 | 71.1 | 0.00109 | 0.00367 | 34.3 |
| 22 | 10,700 | 6.1 | 66.9 | 0.00103 | 0.00343 | 32.5 |
| 23 | 4,850 | 9.1 | 34.8 | 0.00079 | 0.00344 | 14.4 |

Table 1 (continued)

| Run | $N_{Re}$ | $N_{Pr}$ | $N_{Nu}$ | $N_{St}$ | $j$ | $N_{Nu}/N_{Pr}^{0.4}$ |
|---|---|---|---|---|---|---|
| AD 24 | 4,975 | 8.7 | 36.4 | 0.00084 | 0.00355 | 15.3 |
| 38 | 6,920 | 8.8 | 63.3 | 0.00119 | 0.00507 | 26.6 |
| 39 | 7,960 | 8.6 | 72.7 | 0.00106 | 0.00444 | 30.8 |
| 40 | 8,200 | 8.4 | 77.5 | 0.00112 | 0.00464 | 33.1 |
| 41 | 8,965 | 8.3 | 82.0 | 0.00110 | 0.00451 | 35.2 |
| 49 | 17,300 | 5.8 | 106.3 | 0.00107 | 0.00343 | 52.8 |
| 50 | 18,000 | 5.6 | 103.9 | 0.00102 | 0.00323 | 52.0 |
| 51 | 15,280 | 5.6 | 91.8 | 0.00107 | 0.00337 | 46.1 |
| 52 | 16,500 | 5.5 | 95.7 | 0.00106 | 0.00330 | 48.4 |
| 53 | 20,270 | 4.7 | 115.9 | 0.00122 | 0.00342 | 62.5 |
| 54 | 17,750 | 4.6 | 97.7 | 0.00120 | 0.00331 | 53.1 |
| 57 | 22,250 | 4.3 | 118.8 | 0.00123 | 0.00327 | 66.1 |
| 58 | 23,560 | 4.3 | 122.6 | 0.00122 | 0.00321 | 68.6 |
| 59 | 22,760 | 4.3 | 115.5 | 0.00119 | 0.00313 | 64.7 |
| 60 | 24,710 | 4.3 | 123.7 | 0.00117 | 0.00308 | 69.3 |

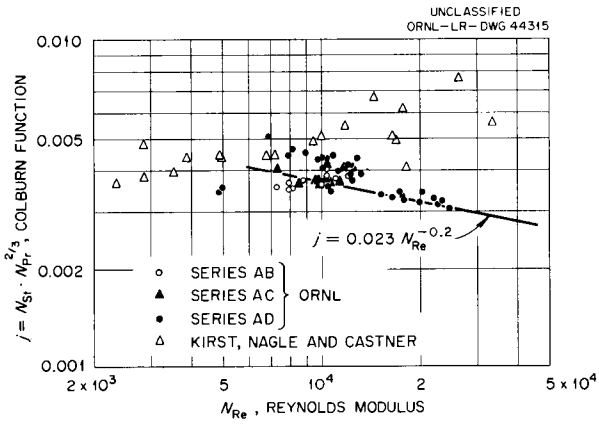


Fig. 8. HTS Heat Transfer.

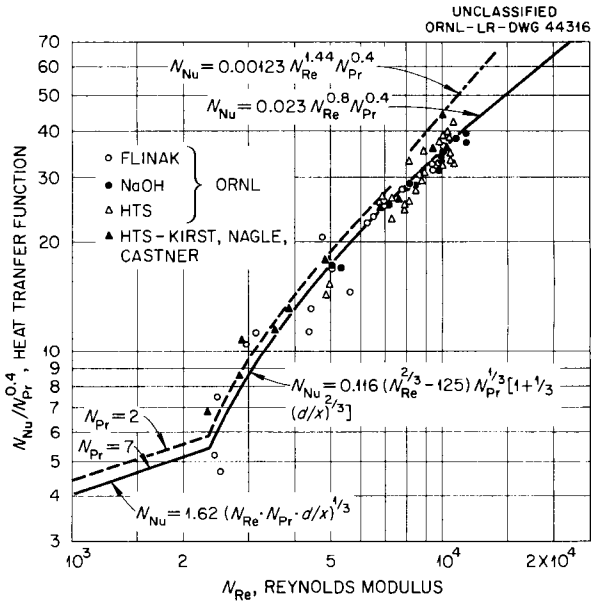


Fig. 9. Comparison of HTS Data for Reynolds Moduli Below 10,000.

empirical [1] correlation of McAdams (*9*) (see Fig. 9),

$$N_{Nu} = 0.023 N_{Re}^{0.8} N_{Pr}^{0.4} , \qquad (6)$$

and the modified equation developed by Colburn (*10*),

$$j = 0.023 N_{Re}^{-0.2} . \qquad (7)$$

Both equations represent heat transfer to "ordinary" fluids ($0.5 < N_{Pr} < 100$) and are applicable under the moderate $\Delta t$ conditions prevailing in this investigation.

[1] Analogy solutions comparing heat transfer and momentum transfer within a fluid flowing turbently in a long tube predict the functional relationships expressed in the empirical correlations (*8*).

## DISCUSSION

The earliest reported data on heat transfer with molten salts are those by Kirst, Nagle, and Castner (*5*) with HTS. Their apparatus consisted

of a 6-ft length of standard $\frac{3}{8}$-in. iron pipe heated by the passage of an alternating electric current in the pipe wall. The molten HTS was pumped through the pipe. Fluid inlet and outlet temperatures were obtained with Chromel-Alumel thermocouples installed in wells at each end of the pipe, and temperatures of the outer surface of the tube were measured at four positions along the pipe. Since the thermal conductivity of HTS was unknown at the time of their study, the results were correlated in the form:

$$\frac{hd}{\mu^{0.4}} = 0.000442\left(\frac{dG}{\mu}\right)^{1.14} \tag{8}$$

over a Reynolds modulus range from 2000 to 30,000. A recalculation (see Appendix C) of the original data [using a recent thermal conductivity value for HTS of 0.35 $\text{Btu}\cdot\text{hr}^{-1}\cdot\text{ft}^{-1}\cdot(°\text{F})^{-1}$ as obtained by Powers (*11*)] yielded the results plotted in Figs. 8 and 9.

while transition begins in the vicinity of a Reynolds modulus of 2300, fully developed turbulent flow is not attained until Reynolds moduli above 6000 are reached. This is shown in Fig. 9, in which the data are presented as the McAdams heat-transfer parameter, $N_{Nu}/N_{Pr}^{0.4}$, for $N_{Re}$ below approximately 10,000. Completely developed turbulence is taken to exist in the region in which the data can be correlated by a line parallel to Eq. (6) (i.e., 0.8 slope). The laminar regime is represented (*14*) by the equation

$$N_{Nu} = 1.62\left(N_{Re}\,N_{Pr}\frac{d}{x}\right)^{1/3}, \tag{9}$$

which is a close approximation to the theoretical relation of Graetz (*15*) for values of $N_{Re}N_{Pr}d/x$ greater than 12.7. A family of curves results, each curve being associated with a specific value of the Prandtl modulus. In the transition region, the Hausen (*16*) equation is shown:

$$N_{Nu} = 0.116(N_{Re}^{2/3} - 125)\,N_{Pr}^{1/3}\left[1 + \frac{1}{3}\left(\frac{d}{x}\right)^{2/3}\right]\left(\frac{\mu_m}{\mu_s}\right)^{0.14}, \tag{10}$$

Kirst, Nagle, and Castner comment with regard to Eq. (8) that the Reynolds modulus appears to the 1.14 power, while 0.8 is the exponent in the most widely accepted heat-transfer equations covering a great variety of fluids over the entire turbulent range. Further, they point out that in the lower portion of this range, say $N_{Re} = 2300$ to 30,000, the data on hydrocarbons break away from the 0.8 exponent line and form a curve in which the exponent varies from 0.8 to 1.4 (*12*). On this basis, they suggest that for $N_{Re} > 35{,}000$ (the upper limit of their data), HTS heat transfer be extrapolated along a line of 0.8 slope.

It is generally accepted that the transition from undisturbed (laminar) flow occurs at a critical Reynolds modulus of about 2300. Under circumstances of elaborately controlled entrance conditions, transition Reynolds moduli as high as 500,000 have been observed with flow in circular tubes (*13*). However, the change from completely laminar to completely turbulent flow is not abrupt, extending over a wide range of the Reynolds modulus above 2300. Thus the results obtained in this Laboratory with HTS, and previously with NaOH and Flinak, indicate for molten salts that,

for $\mu_m = \mu_s$ and Prandtl moduli of 2 and 7. The correlating equation of Kirst, Nagle, and Castner in the form:

$$N_{Nu} = 0.00123N_{Re}^{1.14}N_{Pr}^{0.4} \tag{11}$$

is also given in Fig. 9.

For the region below $N_{Re} = 10{,}000$, the Kirst, Nagle, and Castner data are in substantial agree- with the ORNL results, though somewhat on the high side. Above a Reynolds modulus of 10,000, little agreement is noted (see Fig. 8), and, indeed, the Kirst *et al.* results fall, in the main, outside the ±20% scatter band normally associated with the McAdams equation. The description of the apparatus and procedure by Kirst and his collaborators is too meager to allow more than speculation as to the source of the discrepancy.

The results of earlier studies with NaOH (*3*) and with Flinak (*4*) in stainless steel and nickel tubes are also shown in Fig. 9. The data for Flinak in Inconel tubes have not been included; these are discussed fully in refs (*4*) and (*17*). It suffices to comment that for this combination of salt and container material, the heat transfer was

observed to be a factor of 2 lower than predicted in Eqs. (6) or (7). This difference was found to be directly attributable to a high-melting, insoluble interfacial deposit formed by reaction between Flinak and Inconel. The major constituent of the film was determined to be $K_3CrF_6$. Considering the data scatter normally associated with transition-region heat transfer, the current HTS data agree well with the previous results. Thus the general conclusion that the fused salts, in the absence of phenomena such as surface reaction and/or nonwetting, behave, in a heat-transfer sense, as normal fluids, is further strengthened. On this basis, the standard relations [such as Eqs. (6) and (7)] may be used to describe heat transfer with the molten salts.

It is of some interest to consider the effectiveness of HTS as a coolant in comparison with NaOH and Flinak and with several of the liquid metals. One method for accomplishing such a comparison involves a "cooling-work modulus" (the flow work per unit heat removal), which is a function of the configuration of the system, the nature of the flow, the thermal properties of the fluid, and certain axial and radial coolant-temperature differences. This modulus was derived by Rosenthal, Poppendiek, and Burnett (*18*) for several pertinent combinations of reactor temperature differences. Hoffman (*19*) later extended the analysis to include a symmetrical reactor–heat exchanger complex. The results of such an evaluation are given in Fig. 10. The thermal properties of HTS were extrapolated to 1350°F in order to form a consistent comparison. For the conditions of this calculation (reactor length = 3 ft; ratio of coolant volume to total volume = 0.3; heat generation = 200 Mw or $35.1 \times 10^6$ Btu·hr$^{-1}$·ft$^{-3}$; total $\Delta t$ = 500°F), HTS would appear competitive with bismuth or sodium only at small tube diameters; for a given heat removal, the pumping power required for HTS is ten times that for Flinak.

## CONCLUSIONS

In summarizing this study, the following statements can be made:

1. The HTS experimental results are consistent with data of earlier studies with molten NaOH and Flinak (in the absence of interfacial effects) and, at least in the transition flow region, in agreement with the HTS results of Kirst, Nagle, and Castner.

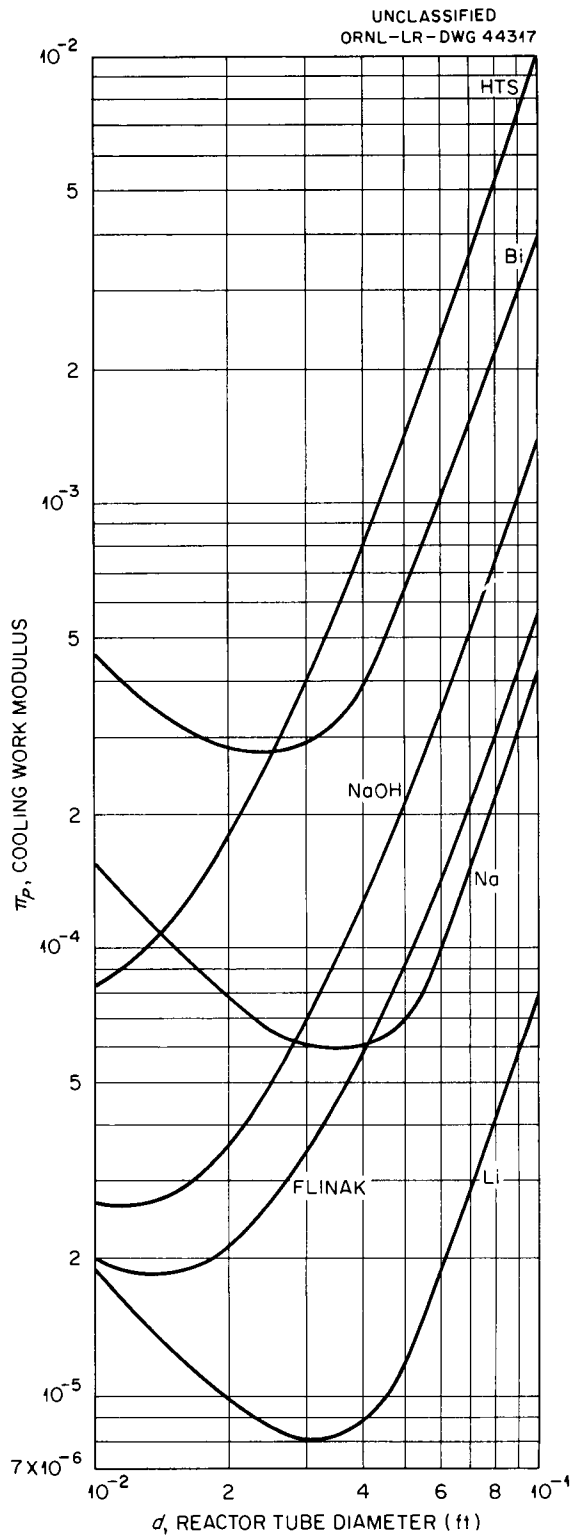


**Fig. 10. Comparison of Coolants.**

2. In a heat-transfer sense, HTS behaves as a normal fluid ($0.5 < N_{Pr} < 100$); and the standard correlations such as those by McAdams, Dittus and Boelter (*20*), and Colburn may be used in designing heat exchange equipment containing HTS.

3. A cooling-effectiveness comparison, assuming a specific set of power generation and temperature conditions, indicates that HTS requires a much greater expenditure of pumping energy to effect a given heat removal than do the other molten salts considered (NaOH and Flinak). Further, HTS appears competitive with the liquid metals (excepting lithium) only at small tube diameters.

4. The relatively excessive pumping power requirements, coupled with the factor of radiation damage, suggest that the use of HTS be restricted to applications other than that of a primary reactor coolant. Areas such as the testing of reactor systems and components under high-temperature, noncorrosive, and nonnuclear conditions appear feasible, in addition to use in secondary coolant circuits of reactors.


## ACKNOWLEDGMENT

The assistance of D. P. Gregory (currently with CANEL Operations of Pratt and Whitney Aircraft) in obtaining the earlier sets of data and the general laboratory support of T. N. Jones and J. Lones are recognized.

## Appendix A

## PHYSICAL PROPERTIES OF HTS

### Density, $\rho$

Values of the density as a function of temperature may be obtained from Fig. 11. This plot is based on measurements made by Kirst, Nagle, and Castner (*5*), using a modified Westphal balance.

### Heat Capacity, $c_p$

A value of 0.373 $Btu \cdot lb^{-1} \cdot (°F)^{-1}$ was obtained for the liquid and 0.32 $Btu \cdot lb^{-1} \cdot (°F)^{-1}$ for the solid. The latent heat of fusion was approximately 35 Btu/lb. These results are based on enthalpy measurements over the range 70 to 1100°F, made by Kirst, Nagle, and Castner (*5*), and checked by Powers (*21*).

### Thermal Conductivity, $k$

A value of 0.35 $Btu \cdot hr^{-1} \cdot ft^{-1} \cdot (°F)^{-1}$ was obtained by Powers (*11*), using a variable-gap device.

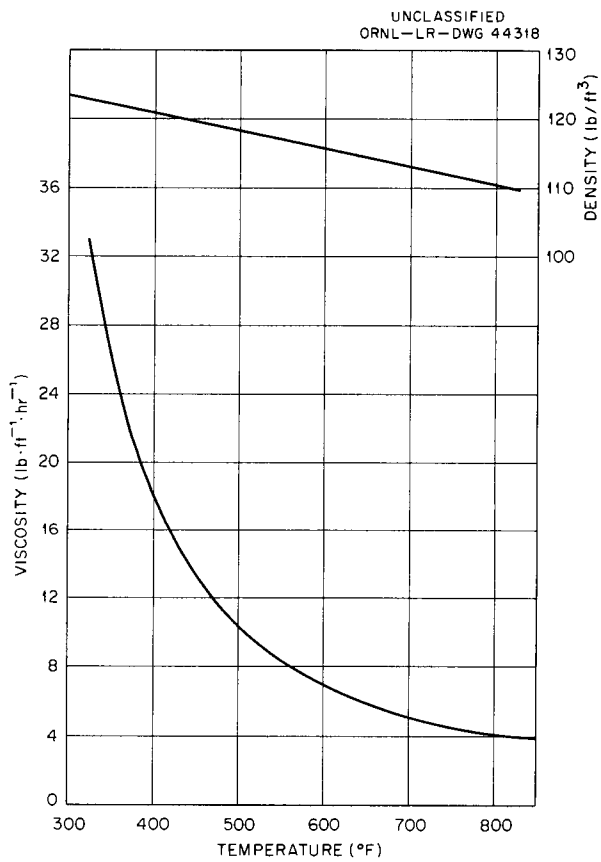


**Fig. 11. Variation of Density and Viscosity of HTS with Temperature.**

### Viscosity, $\mu$

The viscosity was found to vary from about 29 $lb \cdot ft^{-1} \cdot hr^{-1}$ at 340° F to about 4.0 $lb \cdot ft^{-1} \cdot hr^{-1}$ at 800° F (see Fig. 11). Measurements were made by Kirst, Nagle, and Castner (*5*) with a glass Ostwald pipet suspended in a bath of HTS and were checked by Cohen and Jones (*22*), using the same method.

# Appendix B

## EXPERIMENTAL DATA

Table B-1. Experimental Data: Heat-Transfer Studies with Molten HTS

| Run | $t_{m,i}$ (°F) | $t_{m,o} - t_{m,i}$ (°F) | $t_{w,avg}$ (°F) | $t_s - t_m$ (°F) | $w$ (lb/hr) | $G$ (lb·hr$^{-1}$·ft$^{-2}$) | $q_f/A_s$ (Btu·hr$^{-1}$·ft$^{-2}$) | $h$ [Btu·hr$^{-1}$·ft$^{-2}$·(°F)$^{-1}$] | $q_f/q_e$ |
|---|---|---|---|---|---|---|---|---|---|
| | | | | | | $\times 10^6$ | | | |
| AB 6 | 649.7 | 15.3 | 753 | 81.9 | 516 | 2.920 | 91,500 | 1120 | 0.835 |
| 10 | 576.6 | 18.0 | 714 | 105.9 | 690 | 3.905 | 142,000 | 1340 | 0.880 |
| 11 | 595.4 | 11.9 | 688 | 70.5 | 686 | 3.882 | 94,500 | 1340 | 0.876 |
| 17 | 603.6 | 14.4 | 713 | 82.7 | 824 | 4.663 | 137,900 | 1665 | 0.930 |
| 21 | 625.0 | 20.1 | 768 | 113.6 | 600 | 3.396 | 140,000 | 1230 | 0.890 |
| 22 | 654.2 | 20.1 | 784 | 98.5 | 706 | 3.995 | 164,500 | 1670 | 1.035 |
| 29 | 672.8 | 21.0 | 802 | 96.7 | 676 | 3.826 | 164,500 | 1700 | 1.020 |
| 31 | 677.5 | 17.7 | 789 | 82.1 | 774 | 4.380 | 158,000 | 1920 | 1.040 |
| 32 | 693.3 | 18.6 | 806 | 84.7 | 685 | 3.877 | 147,500 | 1740 | 1.000 |
| 34 | 686.2 | 22.7 | 823 | 105.8 | 550 | 3.113 | 144,500 | 1366 | 0.974 |
| AC 10 | 702.9 | 23.5 | 842 | 108.9 | 583 | 3.299 | 158,000 | 1450 | 1.050 |
| 11 | 648.0 | 17.9 | 768 | 90.5 | 733 | 4.148 | 152,000 | 1679 | 0.980 |
| 12 | 656.7 | 11.3 | 734 | 58.1 | 743 | 4.205 | 97,300 | 1671 | 0.956 |
| 13 | 671.1 | 29.9 | 838 | 132.0 | 472 | 2.671 | 163,500 | 1240 | 1.026 |
| 14 | 702.8 | 17.2 | 804 | 80.8 | 516 | 2.920 | 103,000 | 1275 | 1.015 |
| 15 | 705.9 | 17.1 | 805 | 76.8 | 571 | 3.231 | 113,000 | 1470 | 1.005 |
| 16 | 707.0 | 17.7 | 809 | 79.6 | 580 | 3.282 | 118,800 | 1490 | 1.030 |
| 17 | 707.8 | 17.8 | 813 | 79.2 | 665 | 3.763 | 134,000 | 1695 | 1.003 |
| AD 1 | 585.8 | 10.7 | 651 | 46.7 | 908 | 5.140 | 94,700 | 2027 | 0.915 |
| 3 | 595.2 | 9.9 | 661 | 44.4 | 948 | 5.364 | 91,400 | 2059 | 0.865 |
| 4 | 602.7 | 10.3 | 666 | 44.7 | 961 | 5.439 | 96,400 | 2157 | 0.927 |
| 5 | 607.4 | 10.3 | 669 | 43.2 | 974 | 5.513 | 97,700 | 2262 | 0.940 |
| 6 | 611.6 | 9.7 | 671 | 41.5 | 994 | 5.625 | 93,900 | 2263 | 0.925 |
| 7 | 615.0 | 9.4 | 672 | 40.0 | 997 | 5.643 | 91,300 | 2283 | 0.899 |
| 8 | 618.5 | 10.1 | 676 | 39.6 | 1001 | 5.662 | 98,400 | 2486 | 0.940 |
| 9 | 621.5 | 6.8 | 663 | 29.5 | 948 | 5.364 | 62,800 | 2128 | 0.850 |
| 10 | 622.8 | 6.8 | 663 | 27.7 | 948 | 5.364 | 62,800 | 2267 | 0.861 |

Table B-1 (continued)

| Run | $t_{m,i}$ (°F) | $t_{m,o} - t_{m,i}$ (°F) | $t_{w,avg}$ (°F) | $t_s - t_m$ (°F) | $w$ (lb/hr) | $G$ (lb·hr$^{-1}$·ft$^{-2}$) | $q_f/A_s$ (Btu·hr$^{-1}$·ft$^{-2}$) | $h$ [Btu·hr$^{-1}$·ft$^{-2}$·(°F)$^{-1}$] | $q_f/q_e$ |
|---|---|---|---|---|---|---|---|---|---|
| | | | | | | $\times 10^6$ | | | |
| AD 11 | 623.5 | 12.3 | 701 | 54.6 | 948 | 5.364 | 113,600 | 2080 | 0.829 |
| 12 | 627.3 | 13.3 | 707 | 56.4 | 997 | 5.643 | 129,200 | 2291 | 0.927 |
| 13 | 627.4 | 12.6 | 698 | 51.3 | 760 | 4.302 | 93,300 | 1820 | 0.894 |
| 14 | 630.1 | 13.4 | 700 | 50.3 | 750 | 4.246 | 97,900 | 1947 | 0.944 |
| 15 | 632.5 | 13.1 | 701 | 49.1 | 764 | 4.321 | 97,400 | 1984 | 0.956 |
| 16 | 634.5 | 13.2 | 702 | 48.2 | 787 | 4.451 | 101,100 | 2098 | 1.003 |
| 17 | 636.7 | 13.0 | 704 | 48.9 | 711 | 4.023 | 90,000 | 1841 | 0.907 |
| 18 | 638.5 | 13.5 | 710 | 52.4 | 744 | 4.209 | 97,800 | 1867 | 0.941 |
| 19 | 641.1 | 20.5 | 760 | 86.3 | 744 | 4.209 | 148,500 | 1721 | 0.837 |
| 20 | 647.7 | 19.6 | 765 | 86.1 | 731 | 4.136 | 139,500 | 1620 | 0.812 |
| 21 | 653.6 | 19.7 | 769 | 83.7 | 724 | 4.097 | 138,900 | 1660 | 0.810 |
| 22 | 659.7 | 19.6 | 778 | 87.7 | 717 | 4.060 | 137,000 | 1562 | 0.799 |
| 23 | 543.5 | 18.0 | 670 | 104.9 | 486 | 2.749 | 85,000 | 812 | 0.801 |
| 24 | 552.0 | 17.5 | 669 | 96.4 | 481 | 2.720 | 82,000 | 850 | 0.802 |
| 38 | 550.0 | 17.5 | 651 | 77.6 | 673 | 3.807 | 114,700 | 1480 | 0.961 |
| 39 | 558.0 | 15.5 | 648 | 67.2 | 755 | 4.273 | 114,000 | 1697 | 0.962 |
| 40 | 564.0 | 15.5 | 651 | 63.6 | 762 | 4.312 | 115,000 | 1810 | 0.964 |
| 41 | 568.5 | 14.0 | 649 | 58.7 | 824 | 4.662 | 112,400 | 1914 | 0.946 |
| 49 | 679.0 | 15.0 | 773 | 64.8 | 1100 | 6.226 | 160,800 | 2481 | 0.923 |
| 50 | 684.0 | 17.0 | 796 | 76.8 | 1124 | 6.363 | 186,200 | 2425 | 0.879 |
| 51 | 688.5 | 20.0 | 811 | 86.0 | 945 | 5.348 | 184,100 | 2141 | 0.871 |
| 52 | 694.0 | 19.0 | 813 | 82.9 | 1000 | 5.660 | 185,200 | 2233 | 0.872 |
| 53 | 764.5 | 19.0 | 871 | 71.9 | 1051 | 5.946 | 194,500 | 2705 | 0.937 |
| 54 | 776.5 | 20.5 | 890 | 78.8 | 899 | 5.088 | 179,500 | 2279 | 0.857 |
| 57 | 805.0 | 18.5 | 908 | 69.4 | 1067 | 6.038 | 192,300 | 2271 | 0.918 |
| 58 | 812.0 | 17.5 | 911 | 66.2 | 1110 | 6.283 | 189,300 | 2860 | 0.912 |
| 59 | 817.0 | 17.0 | 915 | 65.9 | 1072 | 6.068 | 177,600 | 2695 | 0.862 |
| 60 | 821.0 | 15.5 | 914 | 60.9 | 1164 | 6.589 | 175,900 | 2887 | 0.854 |

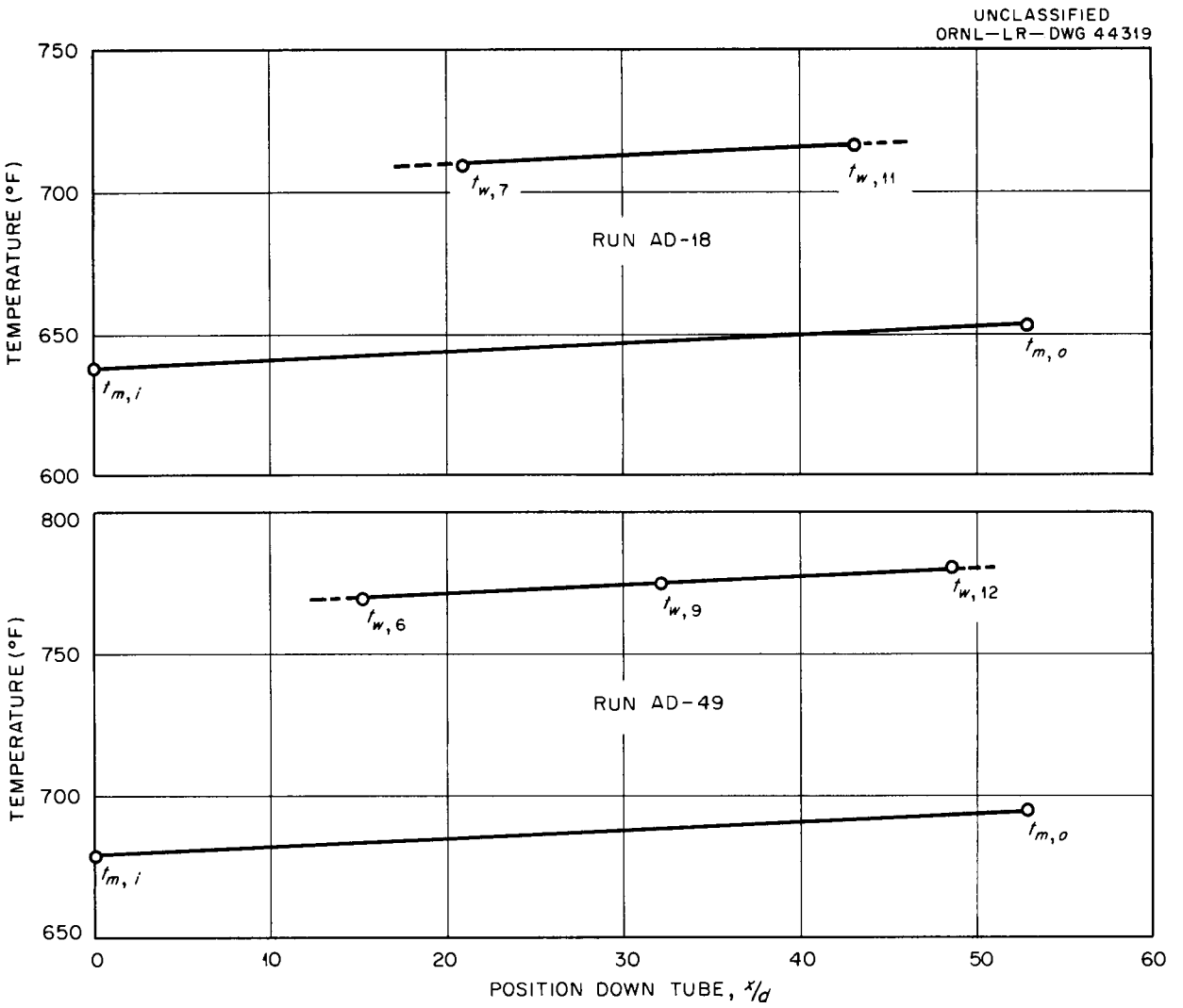


**Fig. 12. Typical Axial Temperature Profiles.**

## Appendix C

### RECALCULATION OF DATA OBTAINED BY KIRST, NAGLE, AND CASTNER

**Table C-1. Results Obtained by Kirst, Nagle, and Castner (5) for Study of Heat Transfer with Molten HTS**

| Run | $N_{Re}$ | $N_{Pr}$ | $N_{Nu}$ | $N_{St}$ | $j$ | $N_{Nu}/N_{Pr}^{0.4}$ |
|---|---|---|---|---|---|---|
| 1 | 16,554 | 5.9 | 166.5 | 0.00155 | 0.00508 | 81.7 |
| 2 | 10,016 | 5.9 | 97.9 | 0.00153 | 0.00501 | 48.0 |
| 3 | 3,517 | 5.5 | 24.7 | 0.00125 | 0.00391 | 12.5 |
| 4 | 2,838 | 6.2 | 19.9 | 0.00113 | 0.00380 | 9.3 |
| 6 | 26,490 | 3.7 | 311.8 | 0.00315 | 0.00759 | 178.8 |
| 7 | 17,174 | 3.7 | 136.6 | 0.00204 | 0.00490 | 78.3 |
| 8 | 11,666 | 3.6 | 77.1 | 0.00171 | 0.00403 | 44.8 |
| 9 | 6,805 | 3.5 | 45.5 | 0.00193 | 0.00442 | 26.9 |
| 10 | 4,872 | 3.5 | 32.7 | 0.00192 | 0.00440 | 19.3 |
| 11 | 33,493 | 3.3 | 279.1 | 0.00250 | 0.00555 | 168.2 |
| 12 | 17,956 | 3.4 | 109.0 | 0.00180 | 0.00403 | 65.3 |
| 13 | 10,380 | 3.4 | 65.4 | 0.00186 | 0.00416 | 39.1 |
| 14 | 7,232 | 3.4 | 47.4 | 0.00197 | 0.00441 | 28.4 |
| 15 | 4,950 | 3.3 | 31.9 | 0.00196 | 0.00435 | 19.2 |
| 16 | 17,856 | 5.7 | 195.5 | 0.00193 | 0.00614 | 95.0 |
| 18 | 2,342 | 6.2 | 15.7 | 0.00108 | 0.00364 | 7.3 |
| 21 | 14,575 | 6.6 | 182.9 | 0.00189 | 0.00666 | 83.3 |
| 22 | 9,448 | 8.2 | 92.9 | 0.00120 | 0.00486 | 39.0 |
| 23 | 3,877 | 8.6 | 34.7 | 0.00104 | 0.00436 | 14.3 |
| 24 | 11,815 | 6.6 | 120.2 | 0.00155 | 0.00544 | 55.0 |
| 25 | 2,872 | 6.4 | 25.4 | 0.00138 | 0.00475 | 11.7 |

## NOMENCLATURE

| | |
|---|---|
| $A_s$ | Heat-transfer surface area, $ft^2$ |
| $c_p$ | Specific heat of fluid at constant pressure, $Btu \cdot lb^{-1} \cdot (°F)^{-1}$ |
| $d$ | Inside diameter of tube, ft |
| $E$ | Voltage impressed on test section |
| $G$ | Mass velocity, lb/hr per square foot of tube cross section |
| $h$ | Coefficient of heat transfer in region of fully developed turbulent flow, $Btu \cdot hr^{-1} \cdot ft^{-2} \cdot (°F)^{-1}$; $h_x$, at position $x$ on tube |
| $I$ | Current passing through test section, amp |
| $k$ | Thermal conductivity of fluid, $Btu \cdot hr^{-1} \cdot ft^{-1} \cdot (°F)^{-1}$; $k_m$, thermal conductivity of test-section tube |
| $q$ | Heat-transfer rate, Btu/hr; $q_f$, heat gain by the fluid; $q_l$, heat loss to the environment; $q_e$, electrical heat input |
| $r$ | Test-section tube radius, ft; $r_s$, inner surface; $r_w$, outer surface |
| $t$ | Temperature, °F; $t_e$, environment; $t_m$, fluid mixed-mean at any position $x$; $t_{m,i}$, fluid mixed-mean inlet; $t_{m,o}$, fluid mixed-mean outlet; $t_{m,avg}$, arithmetic average of inlet and outlet fluid mixed-mean; $t_s$, inner surface of the tube at any position $x$; $t_w$, outer surface of the tube at any position $x$; $t_{w,avg}$, average outer surface of the tube |
| $V$ | Volume of test-section tube wall, $ft^3$ |
| $w$ | Mass flow rate, lb/hr |
| $W$ | Volume heat generation, $Btu \cdot hr^{-1} \cdot ft^{-3}$ |
| $x$ | Distance from test-section tube entrance, ft |
| $x/d$ | Test-section tube length-to-diameter ratio, dimensionless |
| $\mu$ | Absolute viscosity of the fluid, $lb \cdot hr^{-1} \cdot ft^{-1}$; $\mu_m$, evaluated at the fluid mixed-mean temperature; $\mu_s$, evaluated at the temperature of the inner surface of the tube |

### Dimensionless Heat-Transfer Moduli

| | |
|---|---|
| $j$ | Colburn factor, $(hc_p/G)\,(c_p\mu/k)^{2/3}$ |
| $N_{Nu}$ | Nusselt modulus, $hd/k$ |
| $N_{Pr}$ | Prandtl modulus, $c_p\mu/k$ |
| $N_{Re}$ | Reynolds modulus, $dG/\mu$ |
| $N_{St}$ | Stanton modulus, $hc_p/G$ |

## REFERENCES CITED


(1) R. C. Briant and A. M. Weinberg, *Nuclear Sci. and Eng.* **2**, 797 (1957); see also *Molten Fluoride Reactors*, ORNL CF-57-6-69 (June 1957).

(2) H. G. MacPherson, *Molten Salt Reactor Program Status Report*, ORNL-2634 (Nov. 12, 1958).

(3) H. W. Hoffman, *Turbulent Forced Convection Heat Transfer in Circular Tubes Containing Molten Sodium Hydroxide*, ORNL-1370 (Oct. 3, 1952); see also *Heat Transfer and Fluid Mechanics Institute*, p 83, Stanford University Press, Stanford, Calif., 1953.

(4) H. W. Hoffman and J. Lones, ORNL-1777 (Feb. 1, 1955) (classified).

(5) W. E. Kirst, W. M. Nagle, and J. B. Castner, *Trans. Am. Inst. Chem. Engrs.* **36**, 371 (1940).

(6) *Izvest. Vsesoyuz. Teplotekh. Inst. im. Feliksa Dzerzhinskogo* **21**(9), 1 (1952).

(7) H. W. Hoffman, *Physical Properties and Heat-Transfer Characteristics of an Alkali Nitrate-Nitrite Mixture*, ORNL CF-55-7-52 (July 21, 1955).

(8) J. G. Knudsen and D. L. Katz, *Fluid Dynamics and Heat Transfer*, p 407, McGraw-Hill, New York, 1958.

(9) W. H. McAdams, *Heat Transmission*, 3d ed., p 219, McGraw-Hill, New York, 1954.

(10) A. P. Colburn, *Trans. Am. Inst. Chem. Engrs.* **29**, 174 (1933).

(11) W. D. Powers, *ANP Quar. Prog. Rep. Sept. 30, 1957*, ORNL-2387, p 108 (classified).

(12) W. H. McAdams, *Heat Transmission*, 1st ed., p 195–98, McGraw-Hill, New York, 1933.

(13) E. R. G. Eckert, *Introduction to the Transfer of Heat and Mass*, p 66, McGraw-Hill, New York, 1950.

(14) T. B. Drew, H. C. Hottel, and W. H. McAdams, *Trans. Am. Inst. Chem. Engrs.* **32**, 271 (1936).

(15) L. Graetz, *Ann. Physik* **25**, 337 (1885); see also M. Jakob, *Heat Transfer*, p 451, Wiley, New York, 1949.

(16) H. Hausen, *Verfahrenstechnik, Beih. Z. Ver. deut. Ingr.* **1943**(4), 91; see also E. R. G. Eckert and R. M. Drake, Jr., *Heat and Mass Transfer*, McGraw-Hill, New York, 1959.

(17) W. H. Hoffman, *Molten Salt Heat Transfer*, ORNL CF-58-2-40 (Feb. 18, 1958).

(18) M. W. Rosenthal, H. F. Poppendiek, and R. M. Burnett, *A Method for Evaluating the Heat Transfer Effectiveness of Reactor Coolants*, ORNL CF-54-11-63 (Nov. 4, 1954).

(19) H. W. Hoffman, TID-7529 (Part 3) (Nov. 1957) (classified).

(20) W. H. McAdams, *Heat Transmission*, 2d ed., p 167, McGraw-Hill, New York, 1942.

(21) W. D. Powers, *ANP Quar. Prog. Rep. Dec. 10, 1956*, ORNL-2221, p 287 (classified).

(22) S. I. Cohen and T. N. Jones, unpublished data; see also ref (7).

*INTERNAL DISTRIBUTION*

1. L. G. Alexander
2. M. Bender
3. D. S. Billington
4. F. F. Blankenship
5. E. P. Blizard
6. A. L. Boch
7. E. G. Bohlmann
8. C. J. Borkowski
9. G. E. Boyd
10. E. J. Breeding
11. R. B. Briggs
12. R. D. Bundy
13. C. E. Center (K-25)
14. R. A. Charpie
15. J. W. Cooke
16. W. B. Cottrell
17. F. L. Culler
18. L. B. Emlet (K-25)
19. D. E. Ferguson
20. J. Foster
21. A. P. Fraas
22. J. H. Frye, Jr.
23. W. R. Gambill
24. W. R. Grimes
25. B. L. Greenstreet
26. E. Guth
27. D. C. Hamilton
28. C. S. Harrill

29-68. H. W. Hoffman

69. A. Hollaender
70. A. S. Householder
71. T. N. Jones
72. P. R. Kasten
73. G. W. Keilholtz
74. C. P. Keim
75. M. T. Kelley
76. J. J. Keyes, Jr.
77. G. J. Kidd, Jr.
78. B. W. Kinyon
79. A. I. Krakoviak
80. J. A. Lane
81. M. E. Lackey
82. R. S. Livingston
83. J. Lones
84. F. E. Lynch
85. R. N. Lyon
86. H. G. MacPherson
87. W. D. Manly
88. W. B. McDonald
89. J. R. McNally
90. A. J. Miller
91. C. S. Morgan
92. K. Z. Morgan
93. J. P. Murray (Y-12)
94. M. L. Nelson
95. R. H. Nimmo
96. A. M. Perry
97. W. D. Reel
98. P. M. Reyling
99. M. W. Rosenthal
100. G. Samuels
101. H. W. Savage
102. A. W. Savolainen
103. H. E. Seagren
104. E. D. Shipley
105. O. Sisman
106. M. J. Skinner
107. A. H. Snell
108. W. J. Stelzman
109. E. Storto
110. J. A. Swartout
111. E. H. Taylor
112. D. G. Thomas
113. D. B. Trauger
114. F. C. VonderLage
115. J. L. Wantland
116. A. M. Weinberg
117. G. D. Whitman
118. G. C. Williams
119. C. E. Winters
120. J. Zasler

121-123. ORNL Y-12 Technical Library Document Reference Section

124-143. Laboratory Records Department

144. Laboratory Records, ORNL R.C.

145-146. Central Research Library

147. REED Library

## *EXTERNAL DISTRIBUTION*

148. Division of Research and Development, AEC, ORO
149. D. P. Gregory, CANEL Operations, Pratt & Whitney Aircraft, Middletown, Conn.
150-154. S. I. Cohen, Olin Mathieson Chemical Corp., New Haven, Conn.
155. D. H. Groelsema, AEC, Washington, D. C.
156-712. Given distribution as shown in TID-4500 (15th ed.) under Chemistry-General category (75 copies – OTS)